Road Extraction Using SVM and Image Segmentation

Mingjun Song and Daniel Civco

Abstract

In this paper, a unique approach for road extraction utilizing pixel spectral information for classification and image segmentation-derived object features was developed. In this approach, road extraction was performed in two steps. In the first step, support vector machine (SVM) was employed merely to classify the image into two groups of categories: a road group *and a* non-road group. *For this classification, support vector machine (SVM) achieved higher accuracy than Gaussian maximum likelihood (GML). In the second step, the road group image was segmented into geometrically homogeneous objects using a region growing technique based on a similarity criterion, with higher weighting on shape factors over spectral criteria. A simple thresholding on the shape index and density features derived from these objects was performed to extract road features, which were further processed by thinning and vectorization to obtain road centerlines. The experiment showed the proposed approach worked well with images comprised by both rural and urban area features.*

Introduction

Road information not only plays a central role in the transportation application, but also is an important data layer in Geographical Information Systems (GIS). Automated road extraction can save time and labor to a great degree in updating a road spatial database. Various road extraction approaches have been developed. Xiong (2001) grouped these methods into five categories: ridge finding, heuristic reasoning, dynamic programming, statistical inference, and map matching. In ridge finding, edge operators are performed on images to derive edge magnitude and direction, followed by a thresholding and thinning process to obtain ridge pixels (Nevatia and Babu, 1980; Treash and Amaratunga, 2000). Alternatively, gradient direction profile analysis can be performed to generate edge pixels (Gong and Wang, 1997). Ridge points are linked to produce the road segments. Heuristic reasoning is a knowledge-based method in which a series of pre-set rules on road characteristics such as shape index, the distance between image primitives, fragments trend, and contextual information are employed to detect and connect image primitives or anti-parallel linear edges to road segments (McKeown, *et al.*, 1985; Zhu and Yeh, 1986). In the dynamic programming method, roads are modeled with a set of mathematical equations on the derivatives of gray values and select characteristics of roads, such as smooth curves, homogeneous surface, narrow linear features, and relatively constant width. Dynamic programming is employed to solve the optimization problem (Gruen and Li, 1995). In the statistical inference method, linear features are modeled as a Markov point process or a geometric-stochastic model on the road width, direction, intensity and background intensity, and maximum *a posteriori* probability is used to estimate the road network (Barzohar and Cooper, 1996; Stoica, *et al.*, 2000). In a map matching method, existing road maps are used as starting point to update the road network. In general, two steps are involved: first, a map-image matching algorithm is employed to match the roads on the map to the image; second, new roads are searched based on the assumption that they are connected to existing roads (Stilla, 1995). Xiong's classification on road extraction methods is only a generalization, and some other methods may combine different techniques. Active contour models, known as *snakes*, are also used in road extraction (Gruen and Li, 1997; Agouris, *et al.*, 2001). A snake is a spline with minimized energy driven by internal spline and external image forces (Park, *et al.*, 2001). In general, external image forces are represented by the gradient magnitude of an image, which attracts snakes to contours with strong edges. Internal forces are given by a continuity term and a curvature term expressed by the differences of adjacent *snaxels*, which are vertex nodes of the snake, with weights coming from training data, which control the shape and smoothness of the snakes. Through the optimization, the snake evolves from its initial position to desired position with minimized energy. Park and Kim (2001) used template matching to extract road segments in which a road template was formed around the road seed, and an adaptive least squares matching algorithm was used to detect a target window with similar transformation. This method assumes a small difference in brightness values between template and target windows. Most of these road extraction methods require some road seeds as starting points, which are in general provided by users, and road segments evolve under a certain model. Sometimes control points are needed to correct the evolution of roads (Zhao, *et al.*, 2002). Further, these methods use black-and-white aerial photographs or the panchromatic band of high-resolution satellite images and therefore the geometric characteristics of roads alone play a critical role. Boggess (1993) used a classification method incorporating texture and neural networks to extract roads by classifying roads and other features from Landsat TM imagery, but obtained numerous false-inclusions. Roberts, *et al.* (2001) developed a spectral mixture library using hyperspectral images to extract roads, but the use of spectral information alone does not capture the spatial properties of these curvilinear features.

Center for Land use Education and Research, Department of Natural Resources Management and Engineering, The University of Connecticut U-4087, 1376 Storrs Road, Storrs, CT 06269-4087 (mingjun.song@uconn.edu, daniel.civco@ uconn.edu).

In the research reported in this paper, a unique hybrid pixel-object approach was developed using both classification and segmentation to extract road features from Ikonos imagery. Ikonos was launched in September 1999 and is operated by Space Imaging Inc. Ikonos sensors produce four multispectral bands with 4 meter spatial resolution and one panchromatic band with 1 meter resolution. It collects 11-bit data with a wealth of contrast information, which, in combination with geometric characteristics of roads, are particularly useful for road extraction.

Two steps were involved in the proposed approach. First, the image was classified into two groups of features using support vector machine: a *roads group* including actual roads and features which have spectral reflectance similar to roads such as some urban areas, and a *non-roads group* which includes all other features which have spectral values different from roads. Second, the roads-group was masked and partitioned into objects using a region growing image segmentation technique. In this algorithm, a similarity criterion with a higher ratio of shape over spectral information was used. Finally, roads were extracted using the morphological characteristics of the segments.

This paper is arranged as follows: first, support vector machines (SVM) used for classification are described; second, image segmentation used for shape extraction is introduced; third, an experiment showing the proposed approach to extract roads using Ikonos image is presented; and lastly, concluding remarks are offered.

Support Vector Machines

Support vector machine (SVM) is a relatively recent classification technique developed by Vapnik and his group at AT&T BELL Laboratories (Vapnik, 1995; Cortes and Vapnik, 1995). The origin of SVM is the bias-variance tradeoff and over-fitting problem, and it attempts to achieve the best generalization performance by balancing the relationship between the accuracy attained on the training data and the capacity of the machine. It has been applied in fields such as handwritten digit recognition, object recognition, face detection in images, and text categorization (Burges and Schölkopf, 1997; Blanz, *et al.*, 1996; Osuna, *et al.*, 1997; Joachims, 1997). It has been shown that the performance of SVM is as good as or significantly better than that of other competing methods in most cases (Burges, 1998).

The main idea of SVM is to separate the classes with a hyperplane surface so as to maximize the margin among them. SVM is an appropriate implementation of the Structural Risk Minimization principle (Vapnik, 1982) that minimizes the generalization error of a decision function. Based on Vapnik (1995), Osuna, *et al.* (1997) and Burges (1998), SVM is described in three cases as follows: linearly separable, non-separable, and non-linearly separable.

Linearly Separable Case

In this case, because the data set is linearly separable, a hyperplane, defined by $w \cdot x + b = 0$, where x is a point on the hyperplane, w is a n-dimensional vector perpendicular to the hyperplane, and b is the distance of the closest point on the hyperplane to the origin, can be found such that

$$w \cdot x_i + b \geq 1, \quad \text{for } y_i = +1, \text{ and} \tag{1}$$

$$w \cdot x_i + b \leq -1, \quad \text{for } y_i = -1. \tag{2}$$

These two inequalities can be combined into:

$$y_i(w \cdot x_i + b) - 1 \geq 0 \quad \forall i. \tag{3}$$

The problem SVM attempts to solve is to find a hyperplane $w \cdot x + b = 0$ with minimum $\|w\|^2$, subject to constraints (3). It is equivalent to finding the hyperplane with the largest mar-
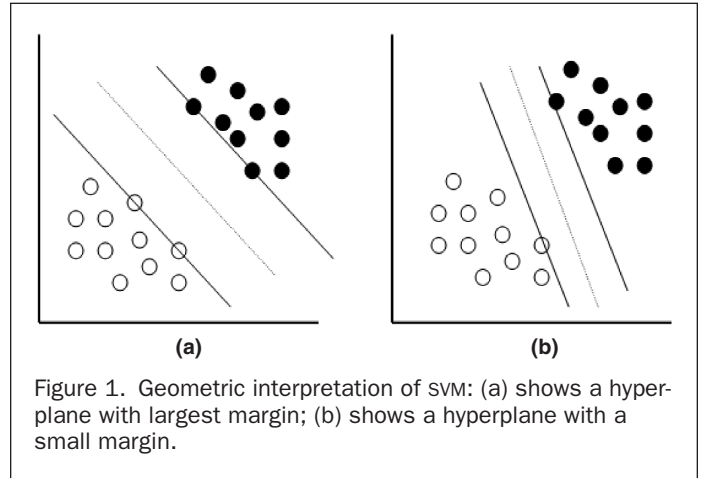

Figure 1. Geometric interpretation of SVM: (a) shows a hyperplane with largest margin; (b) shows a hyperplane with a small margin.

gin, which is defined as the distance between the closest vectors for two classes. Figure 1 shows the geometrical interpretation. The problem can be formulated as follows:

$$\underset{w,b}{\text{Minimize }} \frac{1}{2}\|w\|^2 \quad \text{subject to } y_i(w \cdot x_i + b) - 1 \geq 0$$
$$i = 1, \ldots, l. \tag{4}$$

Using the technique of Lagrange Multipliers, this optimization problem can be formulated into the following quadratic programming problem:

$$\underset{\lambda_1, \ldots \lambda_l}{\text{Maximize }} \sum_{i=1}^{l} \lambda_i - \frac{1}{2} \sum_{i=1}^{l} \sum_{i=1}^{l} \lambda_i \lambda_j y_i y_j x_i \cdot x_j$$

$$\text{subject to } \sum_{i=1}^{l} \lambda_i y_i = 0, \lambda_i \geq 0 \quad i = 1, \ldots, l. \tag{5}$$

The solution of SVM is given by:

$$w = \sum_{i=1}^{l} \lambda_i y_i x_i, \quad b = y_i - w \cdot x_i. \tag{6}$$

The decision function for the classification is given by:

$$f(x) = sign (w \cdot x + b) = sign \left(\sum_{i=1}^{l} y_i \lambda_i (x \cdot x_i) + b \right). \tag{7}$$

In the solution of this problem, those vectors for which $\lambda_i > 0$ are called support vectors, and all other training vectors have $\lambda_i = 0$. It is often found that the number of support vectors is dependent on the intrinsic dimensionality for classification in the training points, not on the dimensionality of the feature vectors; therefore, one does not need to worry about the curse of dimensionality in the support vector machine method (Gualtieri and Cromp, 1998).

Non-Separable Case

For the non-separable case, there does not exist a separating hyperplane, so a set of slack variables ξ_i, $i = 1, \ldots, l$ is introduced in the constraints (3), which changes the objective function to:

$$\frac{1}{2}\|w\|^2 + C \left(\sum_{i=1}^{l} \xi_i \right)^k, \tag{8}$$

where C and k are parameters that define the cost of constraints violation. Again, using the technique of Lagrange Multipliers, the optimization problem becomes:

$$\underset{\lambda_1, \ldots \lambda_l}{\text{Maximize }} \sum_{i=1}^{l} \lambda_i - \frac{1}{2} \sum_{i=1}^{l} \sum_{j=1}^{l} \lambda_i \lambda_j y_i y_j x_i \cdot x_j$$

$$\text{subject to } \sum_{i=1}^{l} \lambda_i y_i = 0, \quad 0 \le \lambda_i \le C, \quad i = 1, \ldots, l. \qquad (9)$$

Non-Linear Case

For the non-linear case, noticing the training data appear in the optimization problem in the form of dot products, one first maps the feature vectors to a higher dimensional Euclidean space by a mapping:

$$\Phi : R^d \, \alpha \, H. \qquad (10)$$

Then, we can get the optimization problem in the space H replacing $x_i \cdot x_j$ by $\Phi(x_i) \cdot \Phi(x_j)$. Suppose there exists a kernel function K such that:

$$K(x_i, x_j) = \Phi(x_i) \cdot \Phi(x_j), \qquad (11)$$

then, we will only need to compute $K(x_i, x_j)$ in the training process. The decision function then becomes:

$$f(x) = sign\left(\sum_{i=1}^{l} y_i \, \lambda_i K(x, x_i) + b\right). \qquad (12)$$

Commonly-used kernel functions are (Osuna, *et al.*, 1997):

Gaussian Radial Basis Function (RBF):

$$K(x, x_i) = \exp\left(-\|x - x_i\|^2\right), \qquad (13)$$

Polynomial with degree d: $K(x, x_i) = (1 + x \cdot x_i)^d$, and $\quad (14)$

Multi-Layer Perceptron (MLP) with values of θ:

$$K(x, x_i) = \tanh(x \cdot x_i - \theta). \qquad (15)$$

In the field of remote sensing, Hermes, *et al.* (1999) used SVM for land use classification with Landsat TM imagery and found that it outperforms maximum likelihood and neural network classifiers. Gualtieri and Cromp (1998) applied SVM to AVIRIS data for hyperspectral image classification and obtained an accuracy of 96 percent for a four-class problem and 87 percent for a 16-class problem. As previously described, the first step of the proposed approach for road extraction was to classify the whole scene into two group features: *road* and *non-road*. SVM was initially designed for binary classification, which obtained good generalization performance through maximizing the margin between two classes. Because each group feature was composed of mixed spectral signatures, the decision boundary should be nonlinear. SVM treats the nonlinear problem by mapping the feature space to a higher dimensional space. Therefore, SVM should be good choice for this first step classification task.

Shape Extraction from Image Segmentation

Classification alone using spectral values cannot extract roads because many other land cover types such as urban areas, especially structures and paved parking areas, have spectral reflectance similar to roads. This entails us to explore the geometric characteristics of the road class. In general, roads are lengthy, narrow, small change-of-curvature objects relative to other land cover features. After the classification is performed, the image is classified into two groups: *roads* and *non-roads*. Inside the roads group, shape information can be used to distinguish roads from similar features such as some urban features (called *false-roads* in this research). Image segmentation provides a powerful tool to extract features such as texture and shape from objects. Image segmentation is a process of partitioning the image into non-intersecting homogeneous regions on neighboring pixels, and no pairs of contiguous regions are homogeneous on the current standard. In the literature review of image segmentation, most techniques can be grouped into three categories: clustering, edge detection and region growing (Haralick and Shairo, 1985; Pal and Pal, 1993). Region growing segmentation starts with an initial partition and regions grow based on certain similarity criteria or optimization of an objective function. This technique seems to be promising because it exploits spatial information, and it should be appropriate for linear object extraction because we could include shape information in the similarity criteria S of region growing, such that:

$$S = r_1 \cdot S_{spec} + (1 - r_1) \cdot S_{shape}, \qquad (16)$$

where S_{spec} represents the similarity of spectral values, S_{shape} represents the similarity for shape features, and r_1 is a ratio coefficient that controls the weights of spectral and shape similarity. Because inside the roads group, all features have similar spectral values, the similarity for shape should have a high weight.

In this research, eCognition® was employed to perform image segmentation to derive objects and shape features. In eCogniton®, image segmentation is performed using a region growing technique based on the similarity criteria of both spectral and shape information and a hierarchical image segmentation is implemented which enables the user to select a satisfying scale of segmentation based on the level of information needed. In eCognition®, shape similarity S_{shape} is expressed by the smoothness similarity S_{smooth} and compactness similarity $S_{compact}$ and a ratio parameter r_2 (between 0 and 1) controlling the weight of S_{smooth} over S_{shape}, and is formulated as follows:

$$S_{shape} = r_2 \cdot S_{smooth} + (1 - r_2) \cdot S_{compact} \qquad (17)$$

Smoothness is described by the shape index *SI*, which is defined as follows:

$$SI = \frac{P}{4 \cdot \sqrt{A}}, \qquad (18)$$

where P represents the border length of the image object, and A is the area of the object.

Compactness is expressed by the density (*DEN*) which is the area of image object divided by its radius approximated by the variability in X and Y coordinate space of all of the object's pixels in the segmented image, and it is implemented as follows:

$$DEN = \frac{\sqrt{N}}{1 + \sqrt{Var(X) + Var(Y)}} \qquad (19)$$

where N is the number of pixels inside the object, $Var(X)$ represents the variance of x-coordinates of all pixels in the object, and $Var(Y)$ represents the variance of y-coordinates.

After the image is segmented, the shape index and density can be derived from resulting objects. Road features should have large values of the shape index, because they have large perimeter and small area, and should have small values of density, because of their small radius. Therefore, roads can be extracted through simple thresholding.

Experiment and Results

Study Area

A subset (700 pixels by 700 pixels, 72°21'34" to 72°23'35" W longitude, 41°39'02" to 41°40'33" N latitude) of an Ikonos image located in Connecticut was selected as the study area, chosen to include both rural and urban features in order to ensure that the proposed approach works well for both natural

Figure 2. 25 April 2000 Ikonos Band 2 image of the study area for road extraction. Space Imaging data provided courtesy of NASA Scientific Data Purchase Program.

Figure 3. Classification result from SVM. White areas represent *roads* group features and black areas represent *non-road* features.

and anthropogenic land covers. The selected Ikonos image was acquired on 25 April 2000 and contained four multispectral bands: blue (0.45–0.52 μm), green (0.52–0.60 μm), red (0.63–0.69 μm), near IR (0.76–0.90 μm) with 4 meter spatial resolution, and one panchromatic band (0.45–0.90 μm) with 1 meter resolution. The image was cloud-free. Figure 2 is a grayscale rendition of Band 2.

Classification

The purpose of classification was to exclude those features that have spectral values different from those of roads. The whole image was classified into two categories (actually two groups): *roads* and *non-roads*. The roads group included those features that had spectral reflectance similar to roads, but when training areas for roads group were selected, only pixels representative of roads were selected, because *false-roads* features would be classified into the roads group during the classification process if they had spectral values similar to roads. This approach would classify as few pixels into the roads group as possible. All other features that had spectral values different from roads would be grouped into the non-roads feature class. Representative areas for these non-road features were selected as training areas. The selection of training areas was done in the NAUTILUS Image Processing System (NIPS) developed by the authors, which provided a multipoint tool for selecting roads points and a polygon tool for selecting other features.

The training data were used to train the support vector machine and the resulting model was used to classify the whole image into two features, shown in Figure 3. For the implementation of SVM, the software package LIBSVM by Chang and Lin (2001) was adapted. Gaussian RBF was used as the kernel function, and parameter C in Equation 8 was set as 10. To evaluate the classification performance of support vector machine, Gaussian maximum likelihood classifier (GMLC) was also used to classify the image. That result is shown in Figure 4. When training areas were selected, 40 percent of the sample data was reserved as test data for evaluating the classification accuracy.
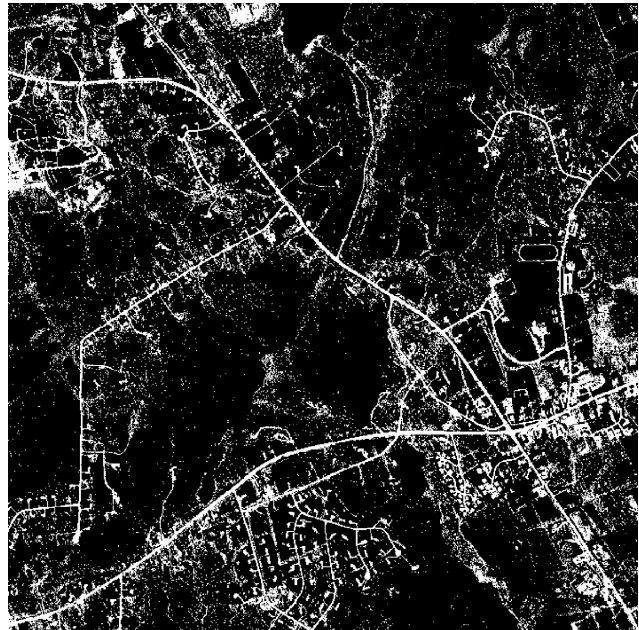

Figure 4. Classification result from GMLC. White areas represent *roads* group features and black areas represent *non-road* features.

Tables 1 and 2 show the classification matrix for SVM and GMLC, respectively.

A comparison of Table 1 with Table 2, and Figure 3 with Figure 4, reveals that SVM produced better results than GMLC. This indicated that the distribution for the feature groups, especially the non-roads class, does not satisfy the normal condition assumed by GMLC, which contributes to the poor performance of GMLC.

TABLE 1. SUPPORT VECTOR MACHINE (SVM) CLASSIFICATION MATRIX

Classification	Reference		
	Roads	Non-roads	User's Accuracy (%)
Roads	94	0	100
Non-roads	2	88	98
Producer's Accuracy (%)	98	100	
Overall classification accuracy = 99%			

TABLE 2. GAUSSIAN MAXIMUM LIKELIHOOD (GML) CLASSIFICATION MATRIX

Classification	Reference		
	Roads	Non-roads	User's Accuracy (%)
Roads	95	7	93
Non-roads	1	81	99
Producer's Accuracy (%)	99	92	
Overall classification accuracy = 96%			

Figure 5. Road features after thresholding. Non-road features have been eliminated.

Road Extraction by Shape Information

After classification, the non-road group features were excluded and a road mask image was obtained for road group features. The road mask image was segmented in the second step. Because there was no significant spectral difference among the road group features, the spectral similarity for image segmentation was less important, and consequently, shape information should weigh more heavily in the similarity criterion. The ratio for shape similarity was set at 0.9, and a scale of 15 reached a satisfactory segmentation for roads through preliminary experiments.

After the road mask image was segmented into objects, the shape index and density were derived using Equations 18 and 19. Examination of the results revealed the shape index for road objects was greater than or equal to 2.3, and density for road objects was less than or equal to 1.1. Finally, a simple thresholding was performed to extract road features, shown in Figure 5.

Road Centerline Extraction and Validation

To this point in the experimental design, roads had been extracted in raster format. In GIS applications, road centerlines in vector format are often more useful. To extract the centerline, two subsequent processes, *thinning* and *vectorization*, were performed on the road features through classification and segmentation.

The thinning process employed here was derived from the field of morphological image processing (Castleman, 1996). It was implemented in a two-pass *erosion* process that is simply defined as a process of eliminating one pixel from the boundary of one object in a binary image. In the first pass, pixels satisfying the condition of a normal erosion were marked as candidates for removal. In the second pass, candidates that would break the connectivity of the object were retained while those that would not were removed (Pratt, 1991). Through the thinning process, all road segments became one-pixel wide. This process was performed in MATLAB®.

After one-pixel wide road segments were derived, a common vectorization procedure could be performed to convert road segments from raster to vector format. This process was

Figure 6. Road centerlines in vector format. Derived from data portrayed in Figure 5.

done using the module of "Grid to Line Coverage" in Arc/Info®. The result is shown in Figure 6.

To validate the proposed approach, the extracted roads were compared to manually digitized roads in the study area developed by Connecticut Department of Transportation. They are both shown in Figure 7 with Ikonos imagery as a backdrop. It can be seen that most roads were extracted correctly including some detailed roads, constructed after the date of the earlier Connecticut DOT aerial photography and

Figure 7. Validation for road extraction. Roads extracted with the methods describe in this paper are displayed in black, and GIS-derived digitized roads are in white and double width. Mis-registration between road layers is due to source material and original projection, yet serve to emphasize differences between the two road layers.

Figure 9. Validation for road extraction of experiment 2. Roads extracted with the methods describe in this paper are displayed in black, and GIS-derived digitized roads are in white and double width. Mis-registration between road layers is due to source material and original projection, yet serve to emphasize differences between the two road layers.

Figure 8. 17 May 2000 Ikonos Band 2 image of second study area, independent test for road extraction. Space Imaging data provided courtesy of NASA Scientific Data Purchase Program.

before the more recent Ikonos imagery, that were not digitized. Some road segments, obscured by shadows or overhanging trees, however, were sometimes omitted using the Ikonos imagery and the techniques described here. These

disjunctions could be solved by manual editing or by a *snapping* program according to the distance and direction of separated two road segments.

To validate further the proposed approach, we selected the second experiment area with a subset of 600 pixels by 600 pixels of another Ikonos image located in Connecticut and acquired on 17 May 2000, shown in Figure 8. Through the same steps as the first experiment, i.e., classification, segmentation, thinning, and vectorization, the validation results shown in Figure 9 exhibit similar performance with those of the first experiment.

Conclusion and Discussion

In this research, a unique hybrid pixel-object approach for road extraction based on classification and segmentation was developed. It is easy to operate yet efficient in road extraction as revealed through the experiment. In the classification stage of extracting *roads* and *non-roads* groups, the support vector machine proved superior to the Gaussian maximum likelihood classifier in classifying mixed features that may not conform to a normal distribution. Binary classification makes it easy to select the training areas, because the user does not need to know what features are in the non-road group category. Region growing image segmentation with the similarity criteria emphasizing shape information works well for road objects in the road mask image. In eCogntion®, there is no mask function when the segmentation is performed, but a mask function would expedite the process of segmentation and remove the possible effect of background. In eCognition®, diagonally connected objects seem not to be recognized as one object, but for the task of road extraction, they should be. This would help extract very narrow roads. A simple thresholding

on shape measurements can extract almost all road features. A thinning process in morphological binary image processing and a common vectorization procedure can be performed on the road features derived using the proposed method to extract road centerline. Further work is suggested to address the development of algorithms or heuristics to fill in road gaps caused by shadow or obscuring land features.

Acknowledgments

References

Agouris, P., S. Gyftakis, and A. Stefanidis, 2001. Dynamic node distribution in adaptive snakes for road extraction, *Vision Interface 2001*, Ottawa, Canada, pp. 134–140.

Barzohar, M., and D.B. Cooper, 1996. Automatic finding of main roads in aerial images by using geometric-stochastic models and estimation, *IEEE Transactions on Pattern Analysis and Machine Intellegence*, 18(7):707–721.

Blanz, V., B. Schölkopf, H. Bülthoff, C. Burges, V. Vapnik, and T. Vetter, 1996. Comparison of view-based object recognition algorithms using realistic 3d models, *Artificial Neural Networks—ICANN'96*, Berlin, pp. 251–256.

Boggess, J.E., 1993. Identification of roads in satellite imagery using artificial neural networks: A contextual approach, *Technical Report: MSU-930815*, Department of Computer Science, Mississippi State University, 46 p.

Burges, C.J.C., 1998. A tutorial on support vector machines for pattern recognition, *Data Mining and Knowledge Discovery*, 2(2): 121–167.

Burges, C.J.C., and B. Schölkopf, 1997. Improving the accuracy and speed of support vector learning machines, *Advances in Neural Information Processing Systems 9*, MIT Press, pp. 375–381.

Castleman, K.R., 1996. *Digital Image Processing*, Prentice Hall, Englewood Cliffs, New Jersey, 667 p.

Chang, C-C., and C-J. Lin, 2001. LIBSVM: A library for support vector machines, Software available at http://www.csie.ntu.edu.tw/~cjlin/libsvm (last date accessed 21 September 2004).

Cortes, C., and V. Vapnik, 1995. Support vector networks, *Machine Learning*, 20:1–25.

Gong, P., and J. Wang, 1997. Road network extraction from airborne digital camera data, *Geographic Information Sciences*, 3(1-2): 51–59.

Gruen, A., and H. Li, 1995. Road extraction from aerial and satellite images by dynamic programming, *ISPRS Journal of Photogrammetry and Remote Sensing*, 50(4):11–21.

Gruen, A., and H. Li, 1997. Semi-automatic linear feature extraction by dynamic programming and LSB-snakes, *Photogrammetric Engineering & Remote Sensing*, 63(8):985–995.

Gualtieri, J.A., and R.F. Cromp, 1998. Support vector machines for hyperspectral remote sensing classification, *27'th AIPR Workshop, Advances in Computer Assisted Recognition, Proceeding of the SPIE, SPIE*, 3584:221–232.

Haralick, R.M., and L.G. Shapiro, 1985. Image segmentation techniques, *Computer Vision*, *Graphics, and Image Processing*, 29:100–132.

Hermes, L., D. Frieauff, J. Puzicha, and J.M. Buhmann, 1999. Support vector machines for land usage classification in Landsat TM imagery, *Proceedings of the IEEE International Geoscience and Remote Sensing Symposium (IGARSS'99)*, Hamburg, 1:348–350.

Joachims, T., 1997. Text categorization with support vector machines, *Technical Report, LS VIII Number 23*, University of Dortmund, ftp://ftp-ai.informatik.uni-dortmund.de/pub/Reports/report23.ps.Z (last date accessed 21 September 2004).

McKeown, D.M., W.A. Harvey, and J. McDermott, 1985. Rule-based interpretation of aerial imagery, *IEEE Transactions on Pattern Analysis and Machine Intelligence*, PAMI-7, No. 5, pp. 570–585.

Nevatia, R., and K. Babu, 1980. Linear feature extraction and description, *Computer Graphics and Image processing*, 13:257–269.

Osuna, E.E., R. Freund, and F. Girosi, 1997. Support vector machines: Training and applications, *A.I. Memo No. 1602, C.B.C.L Paper No. 144*, MIT, 42 p.

Pal, N.R., and S.K. Pal, 1993. A review on image segmentation techniques, *Pattern Recognition*, 26(9):1277–1294.

Park, S., and T. Kim, 2001. Semi-automatic road extraction algorithm from IKONOS images using template matching, *The 22nd Asian Conference on Remote Sensing*, Singapore, 5 p.

Park, H., T. Schoepflin, and Y. Kim, 2001. Active contour model with gradient directional information: Directional snake*, IEEE Transactions on Circuits and Systems for Video Technology*, 11(2):252–256.

Pratt, W.K., 1991. *Digital Image Processing*, 2nd edition, John Wiley & Sons, New York, 720 p.

Roberts, D., M. Gardner, C. Funk, and V. Noronha, 2001. Road extraction using mixture and Q-tree filter techniques, *Technical Report*, National Center for Geographical Information & Analysis, University of California at Santa Barbara, http://www.ncgia.ucsb.edu/ncrst/research/reports/1Q3supplement-p.pdf (last date accessed 21 September 2004).

Stilla, U., 1995. Map-aided structural analysis of aerial images, *ISPRS Journal of Photogrammetry and Remote Sensing*, 50(4):3–9.

Stoica, R., X. Descombes, and J. Zerubia, 2000. A Markov process for road extraction in remote sensed images, *Research Report: RR-3923*, INRIA, Sophia Antipolis, France, http://www.inria.fr/rrrt/rr-3923.html (last date accessed 21 September 2004).

Treash, K., and K. Amaratunga, 2000. Automatic road detection in grayscale aerial images, *ASCE Journal of Computing in Civil Engineering*, 14(1), pp. 60–69.

Vapnik, V.N., 1982. *Estimation of Dependences Based on Empirical Data*, Spring-Verlag, New York, 399 p.

Vapnik, V.N., 1995. *The Nature of Statistical Learning Theory*, Spring-Verlag, New York, 188 p.

Xiong, D., 2001. Automated road network extraction from high resolution images, *NCRST-H white papers*, http://riker.unm.edu/DASH_new/pdf/Application Briefs/Automated Road Network Extraction.PDF (last date accessed 21 September 2004).

Zhao, H., J. Kumagai, M. Nakagawa, and R. Shibasake, 2002. Semi-automatic road extraction from high-resolution satellite image, *Proceedings of Photogrammetric Computer Vision*, Graz, Austria, http://shiba.iis.u-tokyo.ac.jp/member/current/zhao/pub/roadextraction.pdf (last date accessed 21 September 2004).

Zhu, M., and P. Yeh, 1986. Automatic road network detection on aerial photographs, *Proceedings of International Conference on Computer Vision and Pattern Recognition*, Miami Beach, Florida, pp. 34–40.